(2) Reaction with Mullite

Since preliminary corrosion tests showed that mullite reacted with hydrogen gas and that the small amount of glassy phase along grain boundaries had a minimal effect on the reaction rate, the effect of compositional and microstructural variations in the mullite specimens was not determined. The cross section of the mullite sample reacted at 1400°C is shown in Fig. 7. The overall cross section is shown at low magnification Fig. 7(*A*); the central strip is the unreacted mullite core. A high magnification of a section of the right interface showing the reacted layer is shown in Fig. 7(*B*); the reaction front is flat within a few micrometers. The composition profile of the cross section across the reacted surface layer showed no transition layer, in contrast to the glasses with lower Al_2O_3 contents. The silica concentration in the mullite at the interface drops to zero in the α-Al_2O_3 reaction layer.

The weight loss per unit surface area vs time for reactions with H_2 at $T=1350°$ to 1500°C is plotted in Fig. 8. The linear relation indicates that, within the experimental conditions, the alumina residue remains porous and that the transport of reactant and products through this layer is not the rate-limiting step. Furthermore, the composition profile suggests that the reaction is rate-limiting. The 1400°C curve of Fig. 8 plotted in Fig. 2 and the Arrhenius plot of the Fig. 8 data in Fig. 4 provide a comparison of the mullite reaction rate with those for fused silica and the experimental glasses. The activation energy of 389.1 kJ/mol (93.0 kcal/mol) for mullite is near that for silica glass and aluminosilicate glass. The presence of CaO in the aluminosilicate glass lowers the activation energy; as a result, the reactivity of this type of glass appears to be similar to mullite at higher temperatures.

(3) Character of Reacted Zones

The cracks in the reacted glass samples tend to follow the interfaces, as observed in the right specimen of Fig. 5(*A*). The adherence between the unreacted core and the transition layer appears to be better in the left specimen. A higher magnification (Fig. 5(*B*)) of the portion inside the square in Fig. 5(*A*), however, reveals a crack at the interface, as indicated by a bright strip on the sample due to the charging effect on observation by SEM. The concentration profile of the cross section in Fig. 6 also supports this observation. In the case of reacted mullite, however, the cracks go through the reaction interface (Fig. 7), indicating good interfacial adherence between the reacted and unreacted layers.

In all cases, the residue Al_2O_3 layer remains porous and does not halt the reaction. If the Al_2O_3 layers could be sintered into a dense layer, they may act as protective layers. Reacted samples were thus heated to 1600°C for 4 h in air. With aluminosilicate glass, the sintered Al_2O_3 layer cracked into pieces and adhered poorly due to differences in thermal expansion coefficients. With calcium-aluminosilicate glass, a liquid phase formed and rod-shaped mullite grains (confirmed by EDAX) were found growing on the surface.

Because of mullite's greater refractoriness, reacted mullite specimens were sintered at 1650° and 1700° as well as 1600°C. The alumina layer sintered in all of these firings, but cracks were present on observation of the surface by SEM at room temperature. The nature of the cracks, shown in Fig. 9, suggest that cracking occurred on cooling. No further efforts were made in this direction.

IV. Summary

For aluminosilicate (L) and calcium-aluminosilicate (S) glasses, phase separation and crystallization occurred at high temperatures ($\gtrsim$1000°C). After reaction with H_2 gas, the reaction zone consisted of two layers: an intermediate transition layer with an SiO_2 content similar to that of mullite and an outer α-Al_2O_3 residue layer free of SiO_2. Both of these layers were porous. Mullite, on reaction with H_2 gas, had only one reaction layer, consisting only of α-Al_2O_3. The order of decreasing reactivity with H_2 is fused SiO_2, aluminosilicate glasses, mullite, and α-Al_2O_3. The addition of small amounts of CaO to the glasses had little effect, but the reactivity of the glasses approached that of mullite at higher temperatures because of a smaller activation energy. The reaction layers were porous and did not retard the reaction rates under the experimental conditions of the study, indicating that the reaction was the slow step of the overall corrosion process. Sintering of the Al_2O_3 surface layer did not result in a protective layer because of the presence of surface cracks at room temperature which appear to have been formed on cooling because of its higher thermal expansion coefficient. It is of interest to note that, in the case of hydrofluoric acid corrosion, multicomponent glasses are less resistant than SiO_2 glass.[2]

References

[1]S. T. Tso and J. A. Pask, "Reaction of Fused Silica with Hydrogen Gas"; to be published in the *Journal of the American Ceramic Society*.
[2]S. T. Tso and J. A. Pask, "Reaction of Glasses with Hydrofluoric Acid Solution"; to be published in the *Journal of the American Ceramic Society*.
[3]J. F. MacDowell and G. H. Beall, "Immiscibility and Crystallization in Al_2O_3-SiO_2 Glasses," *J. Am. Ceram. Soc.*, **52** [1] 17–25 (1969).
[4]I. A. Aksay and J. A. Pask, "Stable and Metastable Equilibria in the System SiO_2-Al_2O_3," *J. Am. Ceram. Soc.*, **58** [6] 507–12 (1975).

Effect of Variations in Polymerized Oxides on Sintering and Crystalline Transformations

B. E. YOLDAS*

Ceramics and Glasses, Westinghouse Research and Development Center, Pittsburgh, Pennsylvania 15235

This work shows that molecular structural variations can be introduced in oxide systems, including Al_2O_3, ZrO_2, TiO_2, and SiO_2, by controlled hydrolysis and polymerization reactions during the formation of oxides from metal alkoxides. The chemical and stoichiometric makeup of hydroxides and oxides is not fixed and changes rapidly as a function of molecular size in the region where the size is extremely small. It was also observed that internal structural variations significantly alter the sintering behavior of oxide powders and affect their subsequent crystalline transformations.

Received October 5, 1981; revised copy received February 24, 1982.
*Member, the American Ceramic Society.

I. Introduction

METAL ALKOXIDES react with water-forming oxide and hydroxide powders:

$$M(OR)_v + vH_2O \rightarrow M(OH)_v + vROH \quad (1)$$

$$M(OH)_v \rightarrow MO_{v/2} + v/2H_2O \quad (2)$$

where M is a metal with valence v and R is an alkyl C_xH_{2x+1} (n, often used for valence, is used for another purpose in this paper).

Alkoxides of almost any element can be synthesized and their various physical and chemical properties have been extensively investigated.[1–5]

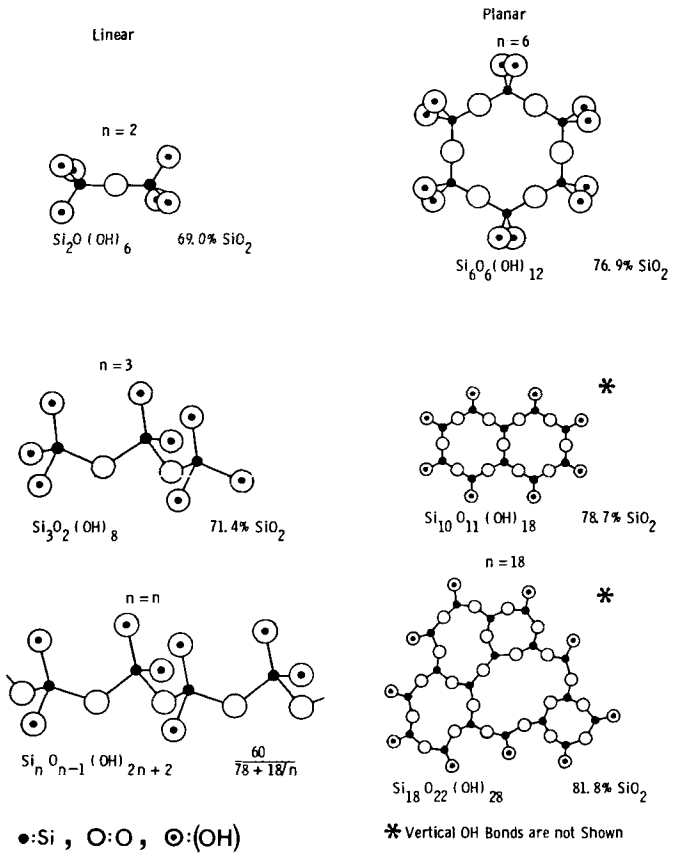

Fig. 1. Schematic representation of effect of molecular size and polymerization type on chemical composition of silicon hydroxide polymers.

The resultant oxide powders sinter to dense bodies at relatively low temperatures due to their extremely small particles.[6] Equations (1) and (2), although often adequate, are overly simplified. For example, formation of hydroxides or hydrates by these processes occurs through two simultaneous reactions: hydrolysis and polymerization.[7]

(1) Hydrolysis

$$\equiv M\text{–}OR + HOH \rightarrow \equiv M\text{–}OH + ROH \tag{3}$$

(2) Polymerization

$$\equiv M\text{=}OH + RO\text{–}M\equiv \rightarrow \equiv M\text{–}O\text{–}M\equiv + ROH \tag{4}$$

where M has a valence of four.

Both reactions occur between "OR" and "OH" groups. However, the latter reaction forms bridging oxygens and leads to eventual condensation of particles by localized network formation. The extent of this localized polymerization, i.e. the size of the particle, depends on the relative rates of the reactions which, in turn, are determined by the type of alkoxide, availability of water, dilution of the system, the reaction temperature, etc. During the initial stages, the relative concentration of bridging oxygens sharply increases at the expense of "OH" and "OR" groups and later becomes relatively stable.[8] This result indicates that the chemical-structural composition of hydroxide polymers is variable when the polymer units are extremely small; thus their properties are also size-dependent. $Si(OR)_4$ can be hydrolyzed such that the equivalent SiO_2 content of the polymers may be varied from <60 to >90% by weight.[8]

II. Experimental Results and Discussion

(1) Formation of Hydroxide Polymers with Variable Oxide Content

In addition to separate hydroxide forms that exist in some oxide systems, e.g. in alumina, it is possible to produce, in almost all systems, hydroxide polymers whose oxide content varies continuously. This result is achieved by controlling the extent and kinetics of hydrolysis and polymerization reactions and ensuring their uniformity. For example, hydrolysis in the silica system,

$$Si(OR)_4 + H_2O \rightarrow Si(OR)_3(OH) + R(OH) \tag{5}$$

rapidly proceeds with further hydrolysis-polymerization, e.g.

$$2Si(OR)_3(OH) + 2H_2O \rightarrow RO\text{–}\underset{\displaystyle OR}{\overset{\displaystyle OH}{Si}}\text{–}O\text{–}\underset{\displaystyle OR}{\overset{\displaystyle OH}{Si}}\text{–}OH + 2ROH, \text{ etc.} \tag{6}$$

to incorporate n silicon ions, i.e. $Si_nO_{n-1}(OH)_{2(n+1)-x}(OR)_x$ (assuming linear polymerization for simplicity). As the reaction proceeds, n increases and x, the number of OR groups, decreases relative to n to a value depending on the hydrolysis temperature and concentration of OR groups in the liquor. Generally, x becomes very small; thus the material can now be treated as essentially organic free-hydroxide polymer and can be expressed as $Si_nO_{n-1}(OH)_{2(n-1)}$. This expression can be generalized as $M_nO_{n-1}(OH)_{(v-2)n+2}$ where M is a metal with valence v.

The oxide content of these linear hydroxide polymers, $M_nO_{n-1}(OH)_{(v-2)n+2}$, would be given by the pyrolysis reaction

$$M_nO_{n-1}(OH)_{(v-2)n+2} \xrightarrow{\text{heat}} n\,MO_{v/2} + \frac{(v-2)n+2}{2}H_2O \tag{7}$$

When M is silicon ($v=4$) the oxide content of the polymer, Q_n, would be

$$Q_n = \frac{n\,SiO_2}{Si_nO_{n-1}(OH)_{(2n+1)}} = \frac{60n}{78n+18} = \frac{60}{78+(18/n)} \tag{8}$$

As the molecules become extremely small, e.g. $n<18$, the oxide content of the overall polymer rapidly drops to the theoretical limit $60/96=61.2\%$ (for $n=1$) corresponding to the monomer hydroxide form, $Si(OH)_4$. When n becomes very large the oxide content approaches the value $60/78=76.9\%$, corresponding to $SiO_2(OH)_2$ which also applies to all closed-ring linear polymers regardless of n. Figure 1 illustrates how the chemical composition varies with polymer size in a silica system.

In reality, when allowed, the polymerization occurs simultaneously in two and three dimensions. In these cases, it becomes very difficult to represent the situation schematically as we have done with linear polymerization. Nevertheless, equations can be written to represent various aspects of these polymers,[9] which are presented elsewhere and summarized in Table I.

In going from linear to planar and three-dimensional polymerization, the connectivity, i.e. average number of bonds connecting each metal ion to another via oxygen, and the maximum oxide content of the polymer, change significantly. In the silica system, the limit for oxide content increases from ≈77% for linear to ≈87 for planar and 100 for three-dimensional polymerization.

As shown in Fig. 2, the size dependence of chemical composition also changes drastically. To achieve 99% of the maximum oxide content requires polymerization of ≈18 silicons in the case

Table I. Chemical Makeup, Oxide Content, and Connectivity of Silica Polymers as a Function of Molecular Size (n)

Polymer Type	Polymer Formula	Connectivity (C_n)	Polymer Oxide Content	Maximum Oxide Content (%) ($n\rightarrow\infty$)	Critical Size* (n_c)
Linear	$Si_nO_{n-1}(OH)_{2n+2}$	$2-\frac{2}{n}$ ($C_\infty=2$)	$\frac{60}{78+\frac{18}{n}}$	76.92	18
Planar**	$Si_nO_{1.5n-(\pi n)^{\frac{1}{2}}}(OH)_{n+2(\pi n)^{\frac{1}{2}}}$	$3-\left(\frac{4\pi}{n}\right)^{\frac{1}{2}}$ ($C_\infty=3$)	$\frac{60}{69+18\left(\frac{\pi}{n}\right)^{\frac{1}{2}}}$	86.96	$\sim 2\times10^3$
3 Dimen.†	$Si_nO_{2n-(\frac{9}{2}\pi n^2)^{\frac{1}{3}}}(OH)_{(36\pi n^2)^{\frac{1}{3}}}$	$4-\left(\frac{36\pi}{n}\right)^{\frac{1}{3}}$ ($C_\infty=4$)	$\frac{60}{60+9\left(\frac{36\pi}{n}\right)^{\frac{1}{3}}}$	100.	4×10^5

* Size Above Which Oxide Content Is Stable Within 1%
** Circular Expansion
† Spherical Expansion

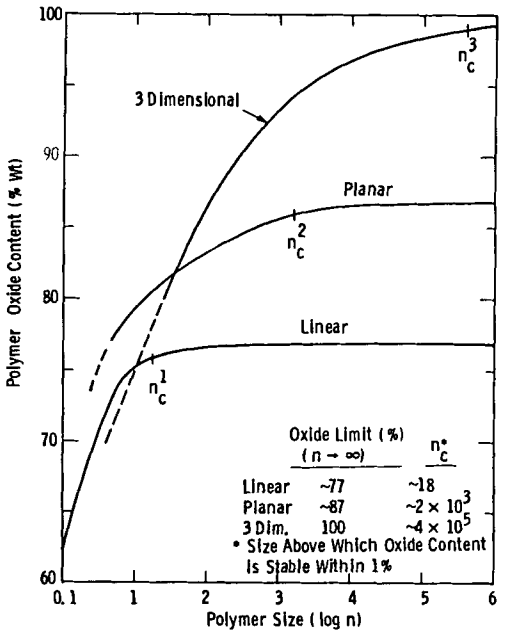

Fig. 2. Effect of molecular size and polymerization type on oxide content of silicon hydroxide polymers.

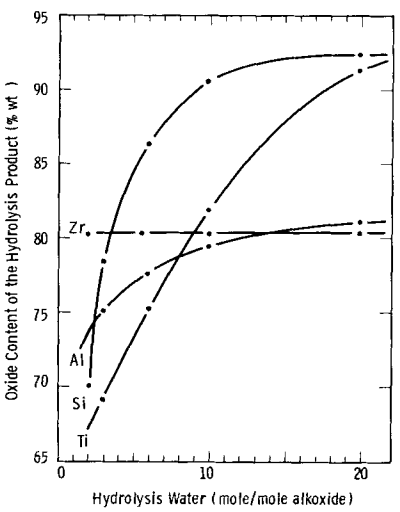

Fig. 3. Change in oxide content of hydroxide as a function of hydrolysis water in various systems (Zr forms a hydrate rather than a hydroxide).

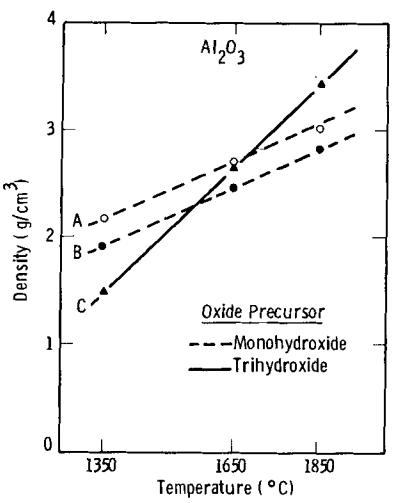

Fig. 4. Temperature dependence of sintering of Al_2O_3 derived from (*A*) amorphous monohydroxide, (*B*) crystalline monohydroxide, and (*C*) crystalline trihydroxide (held 2 h at each temperature).

of linear, $\approx 2\times10^3$ in the case of planar, and $\approx 4\times10^5$ in the case of spherical polymerization (referred as critical size n_c). The last number corresponds to a particle radius of 10 to 15 nm, which is consistent with what is observed by electron microscopy in the case of excess water of hydrolysis. Polymerization apparently proceeds far enough to maximize the oxide content of the molecule. This driving force diminishes as polymerization proceeds, thus limiting the particle size. The questions to be addressed are whether it is feasible to produce hydroxide polymers with low oxide content, ($n < n_c$) and what are the effects of such variations on properties of oxides derived from these precursor polymers.

There are numerous external parameters that affect the hydrolysis and polymerization reactions of metal alkoxides. Three readily controlled, basic parameters affecting the kinetics of these reactions are:

(1) The water/alkoxide ratio, which determines the degree of hydrolysis and nature of initial species formed,

(2) dilution of the reacting species with a neutral solvent which affects the reaction rates and ensures uniformity of the hydrolysis and polymerization throughout the system, and

(3) temperature.

Controlled hydrolysis therefore is best done in a liquid environment where both alkoxide and water are diluted separately in a mutual solvent, i.e. alcohol. In these experiments, only the ratio of hydrolysis water to alkoxide was varied, keeping the dilution of the species constant at a value corresponding to 5 wt% equivalent oxide in the final solution. Hydrolysis products were dried at ≈120° and calcined to 600°C. Figure 3 shows the oxide contents of the polymers as a function of hydrolysis water.

(2) The Alumina System

Aluminum alkoxides, $Al(OR)_3$, hydrolyze vigorously to form aluminum monohydroxides, AlO(OH). Hot-water (>80°C) hydrolysis results in the formation of crystalline boehmite, whereas cold-water hydrolysis produces an essentially amorphous hydroxide.[10] This amorphous hydroxide spontaneously converts to crystalline boehmite when heated to >80°C. It can also convert to trihydroxide by aging at <80°C; this aging requires the presence of water and involves material transport through a dissolution-recrystallization process. Studies of the hydrolysis of aluminum alkoxides and various conversions taking place in this system were presented earlier.[10] AlO(OH), both in amorphous and crystalline form, yields 85% of its weight in aluminum oxide when pyrolyzed to 500°C. Aluminum trihydroxide, $Al(OH)_3$, known as bayerite in crystalline form, yields only 65% in Al_2O_3. Since the internal structures of AlO(OH) and $Al(OH)_3$ are different (for example, coordination of aluminum is four in monohydroxide and six in trihydroxide), the oxides obtained by driving off hydroxyl groups from these hydroxides should also be structurally different. Therefore, an important question is whether this internal structural difference has any influence on sintering of the oxides.

To answer this question, three hydroxides were prepared by hydrolysis of aluminum secbutoxide: (1) a nonliquid hydrolysis by atmospheric moisture, (2) hot-water hydrolysis, and (3) cold-water hydrolysis followed by 24-h aging at room temperature. These processes yield an amorphous monohydroxide, a crystalline monohydroxide, and a trihydroxide, respectively.[10] These hydroxides were then converted to oxide forms by calcining to 600°C and pressed into disks (≈1.6 cm in diam.) under ≈70 MPa. The densification behavior of these samples was observed as they were held for 2 h at various temperatures. The results are given in Table II and Fig. 4.

As shown in Fig. 4, there is a fundamental and important difference in the sintering behavior of the Al_2O_3 obtained from calcination of the trihydroxide and those obtained from monohydroxides. This difference cannot be accounted for on the basis of gross particle size, especially at higher temperatures. (The importance of particle size is significant in the initial stages of sintering and later diminishes as separate particles no longer exist.) Differences between the two oxide powders produced from

Table II. Densification of Aluminum Oxides Obtained Via Hydrolysis of Aluminum Secondary Butoxide

Hydrolysis method	Calcination loss* (wt%)	Density of pressed pellet (g/cm³)	Density (g/cm³) after 2-h heat treatment		
			1350°C	1650°C	1850°C
Hot water (≈80°C)†	≈20	1.01	1.92	2.46	2.84
Air humidity‡	≈41	0.80	2.18	2.71	3.01
Cold-water (≈25°C), 24-h aging in H_2O§	≈30	1.02	1.50	2.67	3.45

*Weight loss of hydrolysis product dried at 120°C on calcining at 600°C. †Results in crystalline AlO(OH). ‡Results in amorphous monohydroxide, which calcines to an amorphous Al_2O_3 at <1000°C. §Results in crystalline $Al(OH)_3$.

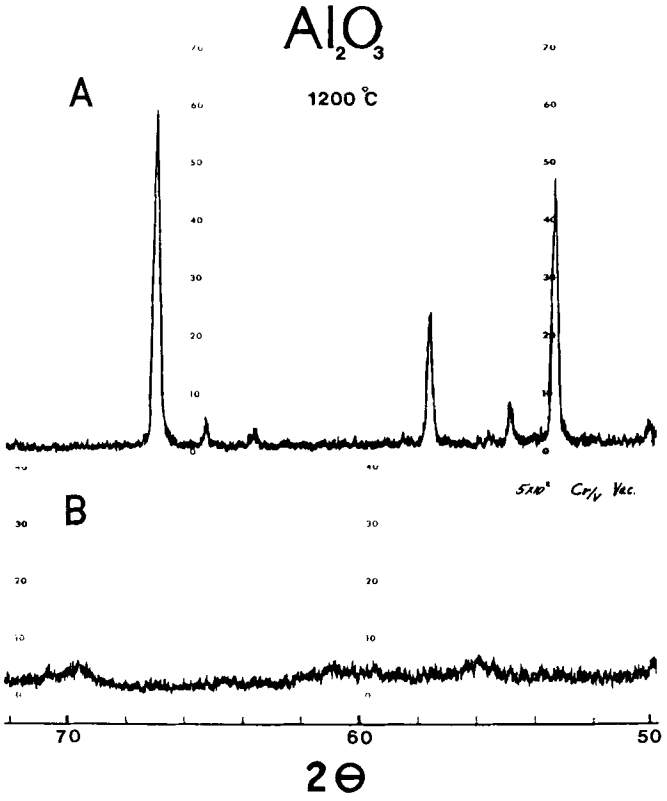

Fig. 5. X-ray diffraction patterns of Al_2O_3 samples obtained by hydrolyzing $Al(OC_4H_9)_3$ with (*A*) 1 and (*B*) 10 moles of water and heating the sample to 1200°C for 30 min (Cr/V$K\alpha$ radiation).

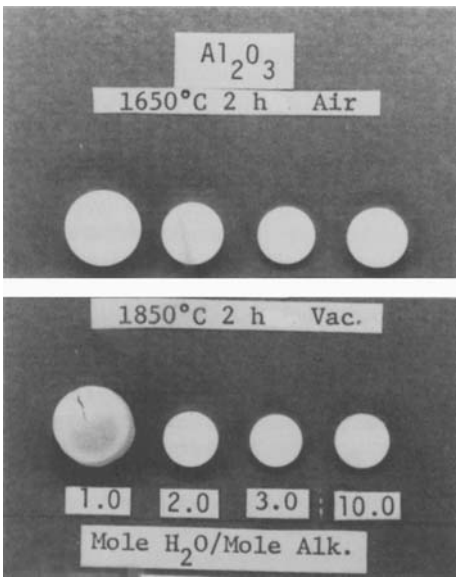

Fig. 6. Variation in shrinkage of Al_2O_3 samples prepared by hydrolysis of $Al(OC_4H_9)_3$ with differing amounts of water.

monohydroxides may, however, be due to the differences in the initial particle size. Nonliquid hydrolysis by atmospheric moisture, besides yielding an amorphous product, is expected to produce very small aluminum monohydroxide polymers. This is because of the limited hydrolysis and reduced mobility of species in the solid state, which greatly restricts the polymerization. The small polymer size is indeed indicated by the higher weight loss of this hydroxide during calcining (Table II).

Apart from these three distinct and well-known forms of aluminum hydroxides, it is possible to produce aluminum hydroxide polymers whose oxide content varies continuously. This is done

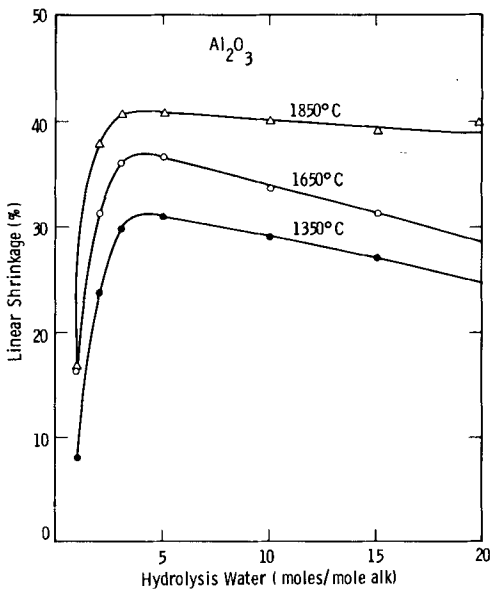

Fig. 7. Effect of hydrolysis water on shrinkage of Al_2O_3 samples produced via hydrolysis of $Al(OC_4H_9)_3$.

by controlled hydrolysis and polymerization reaction in a liquid environment, where both alkoxide and water are dissolved in a mutual solvent, such as an alcohol. In this manner not only can a uniform partial hydrolysis be obtained, but the degree of dilution also allows the extent of interaction of the reacting species to be controlled. Thus, the polymerization and polymer size can be controlled.

To investigate this control, aluminum secbutoxide, $Al(OC_4H_9)_3$, was hydrolized with various amounts of water in secbutyl alcohol. Water and $Al(OC_4H_9)_3$ were separately diluted in alcohol so that the resultant mixture contained 5 wt% equivalent oxide. Bayerite formation was prevented by hydrolyzing at ≈50° and heating the slurries to 100°C immediately after hydrolysis.[10] The appearance of the precipitates in these samples varied considerably as a function of water content. For example, at ≈5 moles water per mole of alkoxide, the volume of precipitate reached a maximum and appeared to be ten times as much as the amount produced by 1 and 20 mole water of hydrolysis. These hydroxides were dried, analyzed, and calcined to oxide at >600°C. When these samples were heated to 1200°C, where transition aluminas convert to α-Al_2O_3, their α-Al_2O_3 conversion behaviors were dissimilar (Fig. 5).

For sintering studies, oxide powders previously calcined at 600°C were pressed into pellets and sintered at various temperatures. Dramatic differences in sample shrinkage after heat treatment are apparent in Fig. 6. The precursor hydroxides formed by 3 to 5 moles of hydrolysis water produced oxides which show the most shrinkage. Thus the structural variations brought about at room temperature during hydrolysis made their effect felt strongly at temperatures as high as 1850°C. One of the most dramatic effects was the degree of resistance shown to sintering by the oxides formed via ≤2 mole water hydrolysis. Samples produced from these oxides showed very little sintering and therefore little shrinkage at all temperatures, including 1850°C (Fig. 7). When the entire heat treatment was done in vacuum, the shrinkage figures did not change significantly. However, samples produced via <3 mole hydrolysis turned black or gray, indicating the presence of organic components or reduction.

Figure 8 shows scanning electron micrographs of fracture surfaces of Al_2O_3 samples obtained via various hydrolysis techniques and sintered at 1350°C. The microstructural differences are considerable in these samples. The sample produced via 1 mole of hydrolysis water consists of sharp-edged particles separated by relatively large spaces. As the hydrolysis water increases to 2 moles, the texture becomes much finer and resembles that of a well-compacted powder. Alumina produced using 5 moles of hydrolysis water has a texture resembling that of a glass. This effect of hydrolysis water, as will be seen, is a characteristic feature in other

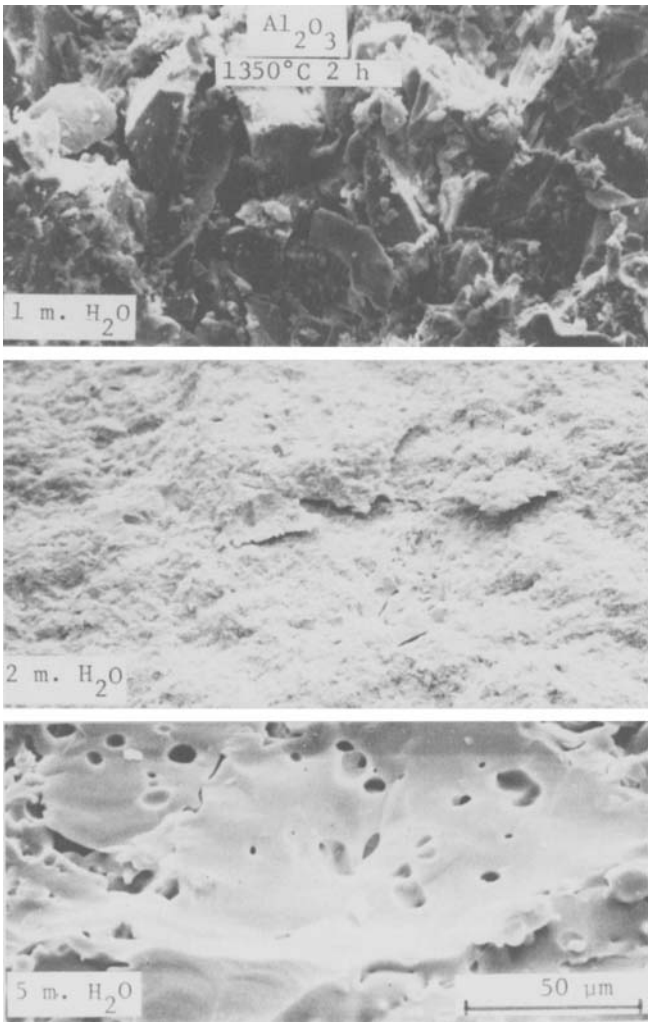

Fig. 8. Scanning electron micrographs of fracture surfaces of Al_2O_3 samples produced via hydrolysis of $Al(OC_4H_9)_3$ with varying amounts of water.

oxide systems as well. Electron micrographs show that alumina produced via low water hydrolysis retains its particulate and fractured appearance, with large intergranular spaces even at 1650°C. The causes of these differences in the microstructure originate during hydrolysis, where not only the amount of water but the temperature of the hydrolysis have a lasting and profound effect. A higher-temperature hydrolysis appears to contribute to the formation of sharply defined separate particles and enhances the resistance to sintering characteristically exhibited by the oxide produced via <2 mole water hydrolysis. What seem to be individual particles (≈2 μm in size) actually are clusters of structural units or polymer regions ≈50 nm in size.

(3) The Zirconia and Titania Systems

There are some important differences between the hydrolysis of aluminum alkoxide and that of zirconium and titanium alkoxides. Zirconium and titanium do not have multiple forms of hydroxides. Indeed, zirconium does not form a hydroxide at all. The zirconium atom does not give up electrons; instead, electrons may either be bound to its ligands covalently or accepted by the zirconium, producing a negative charge[11] which repels hydroxyl groups. This condition leads to preferential formation of oxo and aquo groups rather than true hydroxides.[12] Zirconium and titanium alkoxides and their hydrolysis were investigated by Bradley[1-3] and others. Mazdiyasni *et al.* found that the hydrolysis of zirconium isopropoxide follows at least two steps[5]:

$$Zr(OR)_4 + H_2O \rightarrow ZrO(OR)_2 + R(OH) \quad (9)$$

$$2ZrO(OR)_2 \rightarrow ZrO_2 + Zr(OR)_4 \quad (10)$$

In our experiments, hydrolysis was performed using various amounts of water in a constant dilution in secondary butyl alcohol. Typically a 50% solution of titanium ethoxide, $Ti(OC_2H_5)_4$, and zirconium butoxide, $Zr(OC_4H_9)_4$, was hydrolized with a particular amount of water diluted in butanol such that the equivalent oxide concentration of the final mixture was ≈5% by weight.

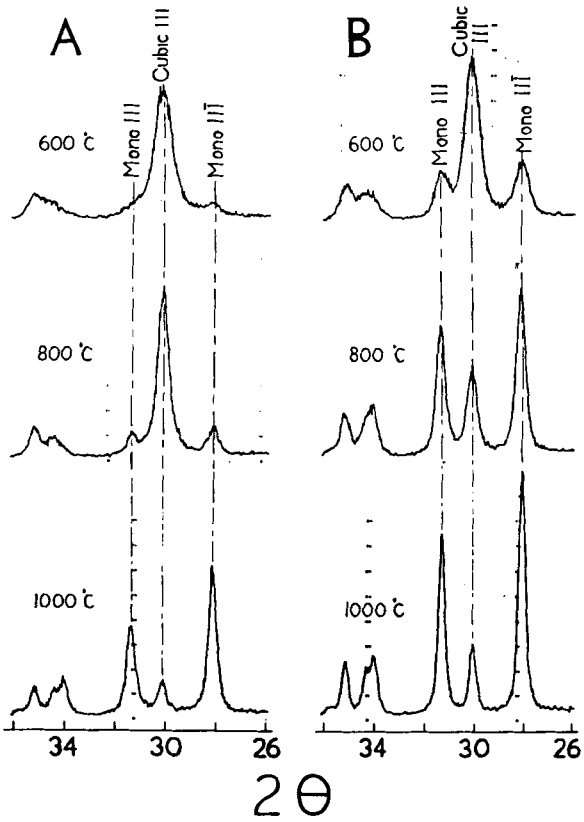

Fig. 9. X-ray diffraction patterns of ZrO_2 powders produced via hydrolysis of $Zr(OC_4H_9)_3$ with (*A*) 1 and (*B*) 10 moles of water and conversion of cubic phase initially formed to monoclinic phase at temperatures indicated for 30 min (Cu$K\alpha$ radiation).

As shown in Fig. 3, the hydrolysis product of zirconium alkoxide contains ≈80% ZrO_2 by weight, regardless of the amount of water used during hydrolysis, corresponding to a composition equivalent to $ZrO_2 - 1.7H_2O$ for the hydrolysis product. The hydrolysis of zirconium alkoxides by atmospheric moisture yields a similar composition. This unique behavior of zirconium is in accordance with the discussion presented above, showing that it does not form true hydroxides. Nevertheless, the amount of water has a substantial impact on the nature of the hydrolysis and polymerization, thus affecting the resultant structure. This is supported by the fact that hardly any precipitate occurs in solutions hydrolyzed with 1 or 2 moles of water per mole of alkoxide; a clear gel forms instead.

The alkoxide structure favors initial formation of an amorphous or cubic ZrO_2 phase, which later converts to tetragonal and monoclinic phases by thermal activation at 600° to 1000°C.[13,14] X-ray investigations of ZrO_2 powder calcined at various temperatures were conducted using Ni-filtered Cu$K\alpha$ radiation. Diffraction patterns were obtained over a wide range of 2θ values, but the emphasis was placed in the $2\theta = 25°$ to 35° range as it contains the two strongest lines of the monoclinic phase at ≈28.3° (11$\bar{1}$) and ≈31.7° (111).[15-17] These studies show significant differences in the ZrO_2 structure as a function of hydrolysis water (Fig. 9). They also indicate that these structural differences strongly influence the subsequent crystalline conversions.

Undoubtedly, further structural studies are required for precise conclusions. Nevertheless, Table III shows the degree to which the structural variations introduced during hydrolysis affect the subsequent transformation to monoclinic phase as calculated from comparison of the cubic (111) peak to monoclinic peaks of (111) and (11$\bar{1}$).

Table III. Effect of Hydrolysis on Monoclinic Phase Transformation of ZrO_2

Hydrolysis water (mol/mol alkali)	Amount of monoclinic phase formed (%)*		
	600°C†	800°C	1000°C
1	14	24	87
10	39	77	86

*Calculated from comparison of cubic (111) peak to monoclinic (111) and (11$\bar{1}$) peaks. †30-min heat treatment.

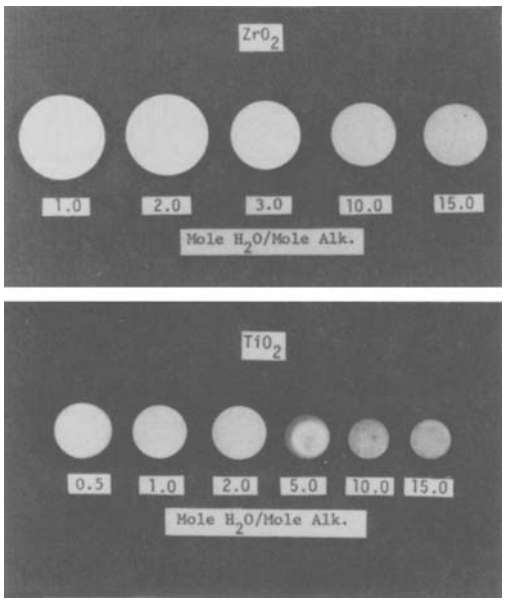

Fig. 10. Variation in shrinkage of ZrO_2 and TiO_2 samples as a function of amount of hydrolysis water (sintered at 1350°C for 2 h).

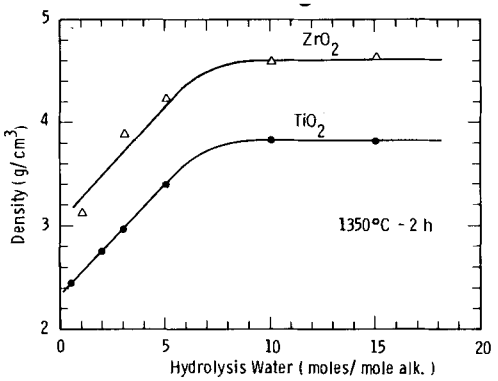

Fig. 11. Effect of hydrolysis water on density of ZrO_2 and TiO_2 powders produced via hydrolysis of $Zr(OC_4H_9)_4$ at $Ti(OC_2H_5)_4$.

The oxide content of the hydrolysis product of titanium alkoxides, unlike zirconium, is strongly affected by the amount of hydrolysis water. Chemical analysis and pyrolysis of the hydrolysis product shows that it contains ≈67% oxide by weight when 2 moles of water are used, and increases to >92% with the use of 20 moles of water. Hydrolysis by atmospheric moisture gives 83% equivalent oxide. Spectral absorption characteristics of these TiO_2 powders show significant variations[18] indicating differences in their molecular structure.

Sintering behavior and densities of ZrO_2 and TiO_2 are again found to be significantly affected by hydrolysis conditions (Figs. 10 and 11). ZrO_2 samples produced via 1 mole H_2O hydrolysis showed no shrinkage and consequently very little coherence at 1350°C, whereas the oxides formed via 10 and 15 moles H_2O hydrolysis shrank considerably, had a glassy appearance, and were very strong. These oxides produced zirconia densities as high as

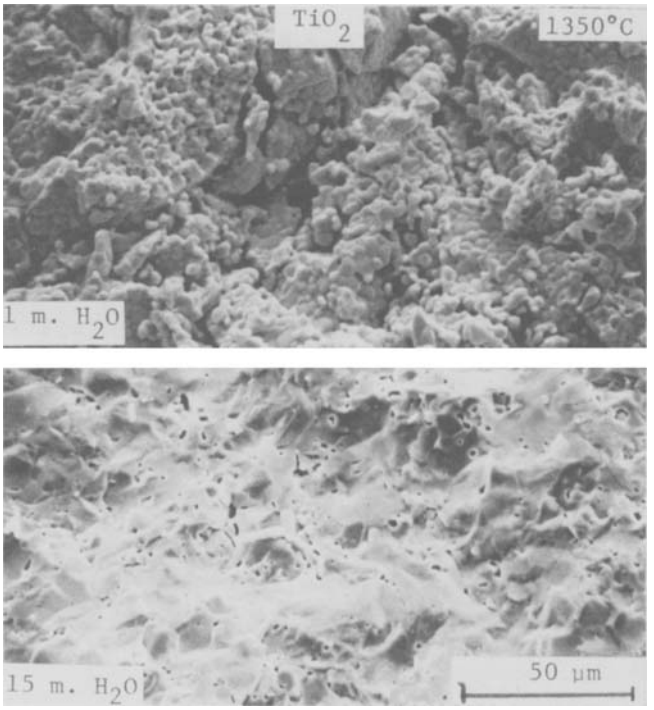

Fig. 12. Fracture surfaces of TiO_2 samples, showing effect of degree of hydrolysis on microstructure.

5.4 g/cm^3 under somewhat higher pressures, e.g. 100 MPa, at 1350°C. Vacuum-firing did not change the result significantly; there was, however, a slight improvement in coherency for the samples hydrolyzed with the lower amounts of water. Scanning electron micrographs of these samples show significant differences in the microstructure. Coarse and separate grains of ZrO_2 produced via 1 mole of hydrolysis water contrast with the denser texture of samples produced via high water hydrolysis.

Titanium oxide sinters to a much greater degree than ZrO_2 at 1350°C. However, the degree of sintering exhibited by these oxides when they are produced via high water hydrolysis is surprising. Their near-molten appearance is shown in the scanning electron micrographs of the fracture surfaces in Fig. 12. When titanium alkoxide is hydrolyzed with a small amount of water, the resultant hydroxides produce sharp, granular oxide particles when calcined. The particles produced via high water hydrolysis, however, have a light, fluffy look, where the boundaries are neither smooth nor sharply defined (Fig. 13). During sintering, polymers coalesce into 1- to 5-μm sized agglomerates which in turn cluster into separate units 20 to 50 μm in size (Fig. 14).

(4) Other Oxides

Similar sintering behavior was noted for numerous other oxides obtained from metal alkoxides, including Y_2O_3, SiO_2, U_2O_5, with slight differences in rate and degree. Among these, the silica system presents a somewhat unusual situation in that the hydrolysis of silicon alkoxides with water produces soluble polymer species which gel into a clear continuous polymer rather than condensing into a particulate precipitate. The reasons for this behavior and the nature of this polymer were presented earlier.[8]

To investigate sintering in the silica system, silicon tetraethoxide, $Si(OC_2H_5)_4$, was similarly hydrolyzed with various amounts of water in alcohol. The hydrolysis product, which is a clear solution in this case, was gelled, dried at 120°C, and calcined to the oxide form at 600°C. The oxide content of the polymers as a function of amount of hydrolysis water can be seen in Fig. 3. As shown, this system can be polymerized to contain >92% oxide by weight at room temperature. The oxide content falls below 70% by weight when the hydrolysis water falls to ≤2 moles. These samples were ground, pressed into disks, and sintered at 1350°C. The sintering behavior was similar to that of the other oxides investigated. However, fast heating causes entrapment of gases and bloating, which must be prevented. In this system, the amor-

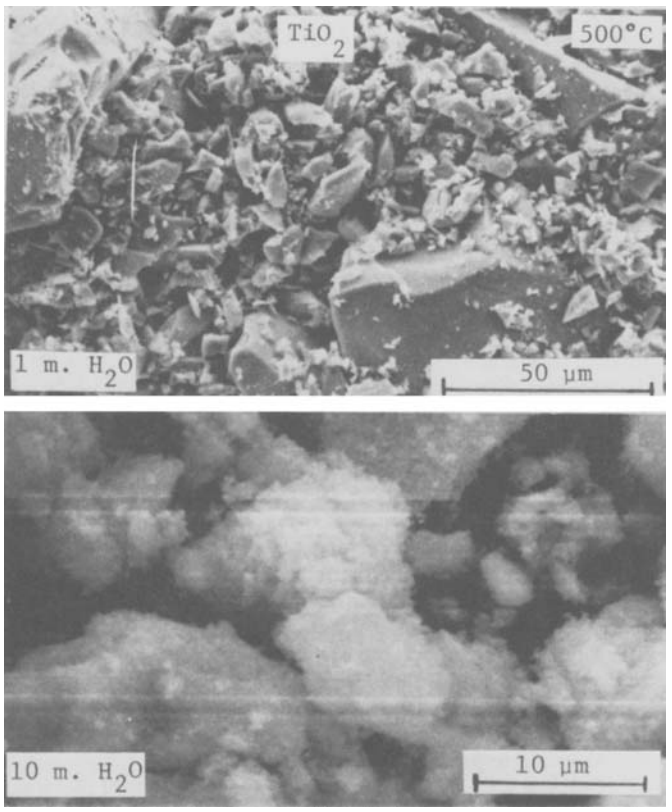

Fig. 13. TiO_2 particles produced by hydrolysis of $Ti(OC_2H_5)_4$ with 1 and 10 moles of water (calcined to 500°C).

phous SiO_2 structures formed by low water hydrolysis tend to be more resistant to crystallization than those formed by high water hydrolysis (Fig. 15).

III. Summary and Conclusions

It was shown that the molecular makeup of the hydroxides and oxides formed via the hydrolysis of metal alkoxides is variable and can be manipulated. It was also demonstrated that these molecular structural variations have a lasting effect on the resultant oxides.

A significant effect of molecular structure on the sintering of oxides is demonstrated by the strikingly different densification behavior of oxides obtained from hydroxide polymers having different chemical and structural makeup. Sintering effects occur as a result of structural differences introduced into the molecular network during hydrolysis and carried onto the oxide state. The view that this phenomenon originates from the molecular structure and stoichiometric parameters is further supported by its effect on crystallization and crystalline transformations. Structural studies show significant differences in structures of polymerized oxides as a function of hydrolysis water, as well as indicating that these structural differences strongly influence subsequent crystalline transformations.

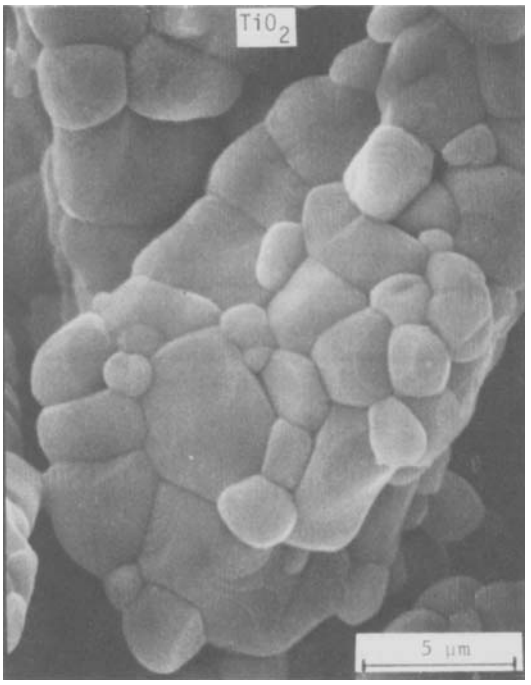

Fig. 14. Agglomerated structure of TiO_2 grains (hydrolysis with 3 moles H_2O, sintered at 1350°C for 2 h).

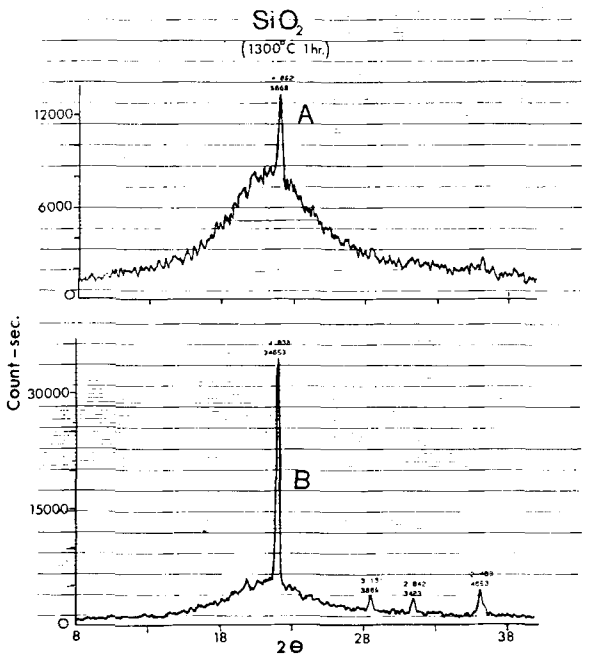

Fig. 15. X-ray diffraction patterns showing differences in crystallization behavior of SiO_2 when it is formed by (*A*) 2 moles H_2O hydrolysis and (*B*) 16 moles H_2O hydrolysis of $Si(OC_2H_5)_4$.

References

[1]D. C. Bradley, R. C. Mehrota, and D. P. Gaur, Metal Alkoxides. Academic Press, NewYork, 1978.

[2]D. C. Bradley and W. Wardlaw, "Zirconium Alkoxides," *J. Chem. Soc.*, 280–85 (1951).

[3]D. C. Bradley; pp. 10–36 in Metal-Organic Compounds, Advances in Chemistry, Series 23. American Chemical Society, Washington, DC, 1959.

[4]R. C. Mehrotra, "Reaction of the Alkoxides of Titanium, Zirconium, and Hafnium with Esters," *J. Am. Chem. Soc.*, **76**, 2266–67 (1954).

[5]K. S. Mazdiyasni, C. T. Lynch, and J. S. Smith, "Preparation of Ultra-High-Purity Submicron Refractory Oxides," *J. Am. Chem. Soc.*, **48** [7] 372–75 (1965).

[6]K. Mazdiyasni, C. T. Lynch, and J. S. Smith II, "Cubic Phase Stabilization of Translucent Yttria-Zirconia at Very Low Temperatures," *J. Am. Ceram. Soc.*, **50** [10] 532–37 (1967).

[7]B. E. Yoldas, "Preparation of Glasses and Ceramics from Metal-Organic Compounds," *J. Mater Sci.*, **12** [6] 1203–1208 (1977).

[8]B. E. Yoldas, "Monolithic Glass Formation by Chemical Polymerization," *J. Mater. Sci.*, **14** [8] 1843–49 (1979).

[9]B. E. Yoldas, "Introduction and Effect of Structural Variations in Inorganic Polymers and Glass Network"; to be published in *Journal of Non-Crystalline Solids*.

[10]B. E. Yoldas, "Hydrolysis of Aluminum Alkoxides and Bayerite Conversion," *J. Appl. Chem. Biotechnol.*, **23** [11] 803–809 (1973).

[11]N. V. Sidgwick, The Electron Theory of Valency. Oxford University Press, London, 1932; p. 273.

[12]W. B. Blumenthal, *The Chemical Behavior of Zirconium*. Von Nostrand, Princeton, NJ, 1958; p. 181.

[13]K. S. Mazdiyasni, C. T. Lynch, and J. S. Smith, "Metastable Transitions of Zirconium Oxide Obtained from Decomposition of Alkoxides," *J. Am. Ceram. Soc.*, **49** [5] 286–87 (1966).

[14]K. S. Mazdiyasni, "Synthesis and Crystalline Growth Mechanism of Submicron Particulates"; pp. 115–25 in Reactivity of Solids. Proceedings of the VI International Symposium on the Reactivity of Solids. January 1969.

[15]G. Teufer, "The Crystal Structure of Tetragonal ZrO_2," *Acta Crystallogr.*, **15** [11] 1187 (1962).

[16]G. M. Wolten,"Direct High-Temperature Single Crystal Observation of Orientation Relation in Zirconia Phase Transformation," *Acta Crystallogr.*, **17** [6] 763–65 (1964).

[17]T. K. Gupta, R. C. Kuznicki, L. H. Cadoff, and B. R. Rossing, "Stabilization of Tetragonal Phase in Polycrystalline Zirconia," *J. Mater. Sci.*, **12** [12] 2421–26 (1977).

[18]B. E. Yoldas,"Introduction of Chemical-Structural Variations in Polymerized Oxides and Its Effect on Sintering and Crystallization"; for abstract see *Am. Ceram. Soc. Bull.*, **61** [3] 372 (1982).